

INTERACTION OF RANDOM WAVES AND CURRENTS

By Terence S. Hedges,¹ Kostas Anastasiou,² and David Gabriel³

ABSTRACT: [The effects of steady, uniform currents on random waves, and the associated water-particle kinematics, are investigated. The basic equations describing the interactions between waves and currents are reviewed, with special reference to the changes in the variance spectra of free-surface displacement and of horizontal water-particle velocity. Theoretical predictions are compared with laboratory measurements of random waves propagating onto an opposing current. The theoretical model is shown to be in reasonable agreement with observations.]

INTRODUCTION

In general, waves do not propagate on quiescent water but travel on currents driven by the tidal forces of the sun and moon, by earth's gravity or by the wind. If the current is positive (i.e., it travels with the waves) then the transformations experienced by random waves as they encounter the current are relatively straight-forward to predict. However, for a negative current (one which opposes the waves) the effects are more complex, owing to the enhanced level of wave breaking induced by the current.

Longuet-Higgins and Stewart (8,9) were the first to deal correctly with the interaction between water waves and currents. They introduced the concept of "radiation stress" and showed the existence of energy transfer between waves and currents. Bretherton and Garrett (1) later drew attention to a quantity which they called "wave action." Wave action is important in the study of waves on currents as, unlike wave energy, it is conserved in the absence of wave generation or dissipation. For linear waves, wave action equals (wave energy density)/(wave frequency relative to the current). Its introduction led to some simplification in the mathematics of wave-current interaction. Instead of employing a relatively complicated energy equation with its physically important radiation stress term, it became possible to allow for the transfer of energy between waves and currents without the need to explicitly calculate the energy exchange. This approach is followed in the present paper.

Wave refraction theory has advanced considerably since introduction of the concept of wave action. The work of Jonsson and others (6,7) involving regular waves has been of particular significance. In the presence of currents it is necessary to distinguish between wave rays and wave orthogonal; wave rays are in the direction of the vector sum of

¹Lect., Dept. of Civ. Engrg., Univ. of Liverpool, Liverpool, L69 3BX, U.K.

²Research Assoc., Dept. of Civ. Engrg., Univ. of Liverpool, Liverpool, L69 3BX, U.K.

³Research Asst., Dept. of Civ. Engrg., Univ. of Liverpool, Liverpool, L69 3BX, U.K.

Note.—Discussion open until August 1, 1985. To extend the closing date one month, a written request must be filed with the ASCE Manager of Journals. The manuscript for this paper was submitted for review and possible publication on June 3, 1983. This paper is part of the *Journal of Waterway, Port, Coastal and Ocean Engineering*, Vol. 111, No. 2, March, 1985. ©ASCE, ISSN 0733-950X/85/0002-0275/\$01.00. Paper No. 19608.

the current and the relative group velocity of the waves, while orthogonals indicate the local orientation of the wave crests. The flux of wave action between neighboring rays determines the wave height.

The interactions of currents with random waves are generally more complicated than the interactions with regular waves. Huang et al. (5) first derived equations describing the changes in wave spectra caused by currents. However, their derivation did not take account of the enhanced level of wave breaking induced by opposing currents, especially associated with the equilibrium range of the spectrum. Tayfun et al. (12) considered the effects on a directional wave spectrum of refraction caused by a combination of varying water depth and current. Hedges (3,4) modified Huang, et al.'s theoretical model to allow for the limit on spectral densities brought about by wave breaking. Unfortunately, up to now, there has been a lack of experimental data against which theories for interaction between currents and random waves could be checked.

In this paper, measurements of random, laboratory-scale waves propagating, without refraction, onto a steady, almost uniform current are reported. Measurements of horizontal water-particle velocities, taken over a range of elevations by using laser-Doppler anemometry, are also described. The results show that Hedges' formulation is in reasonable agreement with observations.

THEORY

The governing equations will be developed with reference to a current traveling in a direction parallel to the wave orthogonals. The formulation may be readily modified to allow for a current flowing at an angle to the direction of wave propagation. However, in that case there will be the added complication of refraction of the waves as they encounter the current.

Consider a train of regular waves (wavelength, L , height, H) traveling on a steady, horizontally and vertically uniform current. The current velocity is U ; U is positive when the current flows with the waves, and negative when it opposes them. In a stationary frame of reference the waves have an apparent angular frequency, ω_a , while in a frame of reference moving along the wave orthogonal at velocity U , the angular frequency is ω_r . Thus

$$\omega_a = \omega_r + kU \dots\dots\dots (1)$$

in which $k (= 2\pi/L)$ = the wave number. In the moving frame of reference, the waves appear to be propagating on "still" water and, therefore, according to linear wave theory, the relative or intrinsic wave angular frequency, ω_r , is given by:

$$\omega_r = (gk \tanh kd)^{1/2} \dots\dots\dots (2)$$

In the preceding expression, g = gravitational acceleration; and d = the water depth.

If a fixed vertical plane, normal to the wave orthogonal, is a distance, x , from the origin of the stationary co-ordinate system, then its distance, x_r , from the origin of the moving co-ordinate system may be written:

$$x_r = x - Ut \dots\dots\dots (3)$$

in which t = time ($x_r = x$ at $t = 0$).

In the moving frame of reference the displacement, η , of the water surface from mean-water-level (MWL) is given by linear wave theory as:

$$\eta = \frac{H}{2} \cos(kx_r - \omega_r t) \dots\dots\dots (4)$$

However, as a result of Eqs. 1 and 3, this expression may be rewritten as:

$$\eta = \frac{H}{2} \cos(kx - \omega_a t) \dots\dots\dots (5)$$

Furthermore, in the moving frame of reference the horizontal component of water-particle velocity at an elevation, z , above mean-water-level is:

$$u_r = \frac{H}{2} \omega_r \frac{\cosh k(d+z)}{\sinh kd} \cos(kx_r - \omega_r t) \dots\dots\dots (6)$$

The horizontal component of water-particle velocity in the stationary frame of reference is

$$u_a = U + u_r \\ = U + \frac{H}{2} (\omega_a = kU) \frac{\cosh k(d+z)}{\sinh kd} \cos(kx - \omega_a t) \dots\dots\dots (7)$$

As before, use has been made of Eqs. 1 and 3 to eliminate ω_r and x_r from the preceding expression.

When waves travel from one current region to another there will be no change in the apparent frequency, ω_a . However, there will be changes in the relative wave frequency, in the wavelength and in the wave height. The changes in ω_r and L (or k) may be found from Eqs. 1 and 2 while the change in H is determined from the principle of wave action conservation (1):

$$\frac{\partial}{\partial x} \left[\frac{E(U + C_{gr})}{\omega_r} \right] = 0 \dots\dots\dots (8)$$

in which E ($= \rho g H^2 / 8$) = the wave energy density; C_{gr} = the relative group velocity of the waves; and ρ = water density. For waves traveling from quiescent water onto a current, an equivalent form of Eq. 8 is

$$\frac{E_0 C_{g0}}{\omega_a} = \frac{E(U + C_{gr})}{\omega_r} \dots\dots\dots (9)$$

in which the subscript "0" refers to quantities in the zero-current area; and C_{g0} = the wave group velocity in this area. Again, the quantities C_{gr} and ω_r refer to the coordinate system moving with the current velocity, U . According to linear wave theory

$$C_{g0} = \frac{1}{2} \left(1 + \frac{2k_0 d}{\sinh 2k_0 d} \right) \frac{\omega_a}{k_0} \dots\dots\dots (10)$$

and

$$C_{gr} = \frac{1}{2} \left(1 + \frac{2kd}{\sinh 2kd} \right) \frac{\omega_r}{k} \dots \dots \dots (11)$$

In addition to predicting the change in the energy density of regular waves, Eq. 9 may also be used to describe the effects of currents on long-crested random waves. In this case, the value of ω_a of each component of the random sea will remain constant as the waves cross from the quiescent area into the current region. Consequently, the spectral density of free-surface displacement for the current region, $S_{\eta\eta}(\omega_a, U)$, is related to the value in the quiescent area, $S_{\eta\eta}(\omega_a)$, by:

$$\frac{S_{\eta\eta}(\omega_a, U)}{S_{\eta\eta}(\omega_a)} \left[= \frac{S_{\eta\eta}(\omega_a, U)d\omega_a}{S_{\eta\eta}(\omega_a)d\omega_a} = \frac{E}{E_0} \right]$$

$$= \frac{\omega_r \left[1 + \left(\frac{2k_0d}{\sinh 2k_0d} \right) \right]}{2k_0 \left\{ U + \left[1 + \left(\frac{2kd}{\sinh 2kd} \right) \right] \frac{\omega_r}{2k} \right\}} \dots \dots \dots (12)$$

If the water depth is sufficiently great that all components of the random sea, both in the quiescent area and in the current region, are propagating on deep water, then

$$\frac{S_{\eta\eta}(\omega_a, U)}{S_{\eta\eta}(\omega_a)} = \frac{\omega_r^2}{\omega_a^2} \frac{1}{\left(1 + \frac{2U\omega_r}{g} \right)} = \frac{1}{\left(1 + \frac{U\omega_r}{g} \right)^2 \left(1 + \frac{2U\omega_r}{g} \right)}$$

$$= \frac{4}{\left[1 + \left(1 + \frac{4U\omega_a}{g} \right)^{1/2} \right]^2 \left(1 + \frac{4U\omega_a}{g} \right)^{1/2}} \dots \dots \dots (13)$$

Eq. 13 was first given by Huang et al. (5). Based upon Eq. 12, it is subject to the same set of assumptions, one of which is that the waves are not refracted by the current. In general, as waves propagate onto an opposing current they tend to shorten and increase in height. Consequently, $S_{\eta\eta}(\omega_a, U)$ increases and Eq. 13 predicts that it will become infinite when $\omega_a = -g/4U$; the energy of the particular component waves cannot propagate onto the current and wave breaking will occur at the current boundary. However, even components which do propagate onto the current may still be affected by breaking because there is a limit to which waves can grow in any particular frequency band (11). For deep water, this "equilibrium range constraint" has been given by Hedges (3) as follows:

$$S_{\eta\eta ER}(\omega_a, U) = \frac{A^*g^2}{(\omega_a - kU)^5} \cdot \frac{1}{\left[1 + \frac{2U(\omega_a - kU)}{g} \right]} \dots \dots \dots (14)$$

in which "ER" refers to the equilibrium range; and A^* = a numerical constant. Note that in the absence of a current, Eq. 14 reduces to the more usual form derived by Phillips (11); for that case, Phillips quotes values for A^* in the range 0.008–0.015. Provided that the equilibrium range of the spectrum is associated with deep water, it is assumed that Eq. 14 will apply in the calculation of spectral densities for the current region whenever $S_{\eta\eta ER}(\omega_a, U)$ is less than $S_{\eta\eta}(\omega_a, U)$ given by Eq. 12 (or 13).

Once the spectrum of free-surface displacement has been established for the current area, then the corresponding spectrum for the horizontal component of water-particle velocity may be predicted using Eq. 7:

$$S_{uu}(\omega_a, U) = (\omega_a - kU)^2 \frac{\cosh^2 k(d+z)}{\sinh^2 kd} \cdot S_{\eta\eta}(\omega_a, U) \dots \dots \dots (15)$$

EXPERIMENTAL WORK

Description of Apparatus.—Experiments were performed in a random wave flume in the Civil Engineering Department at the University of Liverpool. The flume is 15.25 m long, 0.60 m wide with an operating water depth of 0.45 m. It is constructed so that waves are generated on quiescent water and then propagate into an opposing current (see Fig. 1). The current is introduced through the beach and removed through louvres approximately half-way along the flume. The beach has a slope of about 1:6 and consists of a layer of rubberized matting overlying a wooden slab bored with a regular pattern of holes through which the current may pass. The current velocity can be varied by controlling the discharge of the pumps.

The previous configuration, although convenient and easy to operate, did not initially produce currents which were sensibly uniform with depth. This condition was not achieved until the foot of the beach had been raised slightly, to increase flow along the floor of the flume, and a high surface current had been suppressed by covering the upper part of the

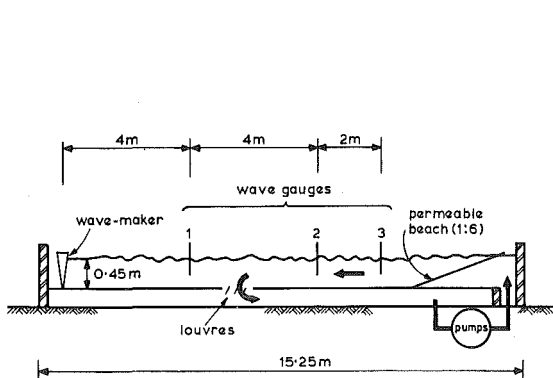


FIG. 1.—Schematic Diagram of Wave-Current Flume

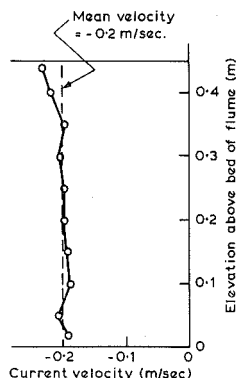


FIG. 2.—Measured Current Profile at Wave Gage 2

beach with an impermeable plate. Unfortunately, it was more difficult to suppress the turbulence in the current, partly generated by the pumps but also produced by the flow through the beach. The problems caused by the turbulence, in analyzing the data from the experiments, are examined later.

The wave-maker indicated in Fig. 1 has a paddle which is hinged at the floor of the flume. It is driven by a control signal from a minicomputer and, while generating waves, it is able, simultaneously, to absorb reflections from the beach or other sources. This it achieves through the use of a feedback signal from a transducer measuring the force on the face of the paddle.

Water-surface displacements were measured with resistance-type wave gages while water-particle velocity measurements were collected using a laser-Doppler anemometer. The anemometer was operated in forward scatter mode and was capable of resolving velocities in two directions, at right angles to one another.

Experimental Procedure.—Four different variance spectra of free-surface displacement were used in the test program. The first spectrum was of the Pierson-Moskowitz type, described by the equation

$$S_{\eta\eta}(\omega_a) = \frac{0.0081 g^2}{\omega_a^5} \exp \left[\frac{-0.74 \left(\frac{g}{W} \right)^4}{\omega_a^4} \right] \dots \dots \dots (16)$$

in which W = the wind speed. The value of W simulated in the tests was 1.3 m/s, the spectrum having a peak at 6.62 rads/s. The corresponding significant wave height was 0.036 m.

The second and third spectra were of the JONSWAP form:

$$S_{\eta\eta}(\omega_a) = \frac{A g^2}{\omega_a^5} \exp \left(\frac{-1.25 \omega_{pk}^4}{\omega_a^4} \right) \cdot \gamma^r \dots \dots \dots (17)$$

in which $A = 5.78 [H_s(\omega_{pk}/2\pi)^2]^{2.036} (-0.298 \ln \gamma + 1.0)$; and $r = \exp(-(\omega_a - \omega_{pk})^2/2\sigma^2\omega_{pk}^2)$; in which $\sigma = 0.07$ for $\omega_a \leq \omega_{pk}$ and $\sigma = 0.09$ for $\omega_a > \omega_{pk}$.

H_s is the significant wave height, γ is the peak enhancement factor, and ω_{pk} is the peak frequency. The JONSWAP spectra had $H_s = 0.036$ m (i.e., the same as for the Pierson-Moskowitz spectrum), $\gamma = 6.0$, and peak frequencies of 7.95 and 6.62 rads/s, respectively. The corresponding values of A were 0.0081 and 0.0038.

The fourth spectrum used in the tests merely described the Pierson-Moskowitz equilibrium range between lower and upper cut-off frequencies, 5.7 rads/s and 25.0 rads/s:

$$S_{\eta\eta}(\omega_a) = \frac{0.0081 g^2}{\omega_a^5} \dots \dots \dots (18)$$

The corresponding significant wave height for this spectrum was 0.054 m.

The control signals for the wave-maker were generated digitally on the Departmental mini-computer. The method used was based upon the linear superposition of a finite number of sinusoidal components each

acting at a certain frequency and having a random phase. These random phases were uniformly distributed between 0 and 2π . By virtue of the Central Limit Theorem of statistics, the water-surface displacement produced in this manner obeys a mean-zero Gaussian probability distribution. Therefore, the method used for the generation of the control signal was consistent with the theoretical framework of first-order random wave theory. For each target spectrum the cumulative distribution of variance was calculated and⁹ was split into sixty slices. Forty slices of equal area covered the 15% of the total variance at the high frequency end of the distribution, with the remainder of the distribution being covered by the other twenty slices, again of equal area. Each sinusoidal component was taken to act at the middle of the frequency band corresponding to its slice of the total variance. [For a more detailed description of the generation of random signals with a target spectral density, see Borgman (2)].

The records produced as control signals were 12,000 points long with a digitizing interval of 0.05 sec. They were passed through a digital to analogue converter and the resulting voltage signals stored on an F.M. tape deck. The analogue signals were later replayed into the wave-maker control console while the histories of free-surface displacement and particle velocities were sampled on-line and stored on magnetic disk, for subsequent off-line analysis.

During the experiments, the mean water depth at the wave-maker was kept at 0.45 m and free-surface displacement was monitored at three positions along the flume: at 4.0 m, 8.0 m and 10.0 m from the paddle (Fig. 1). Horizontal and vertical components of water-particle velocity were measured at the second of these positions, at elevations of -0.5 mm, -225 mm and -400 mm, relative to MWL. The mean current velocity during the tests was 0.2 m/s (Fig. 2). With the current alone flowing, the mean-water-level at wave gage 2 was approximately 1 mm below that at the paddle. Addition of the waves caused little noticeable change either to MWL or to the current.

Nine records were collected at each of the three elevations at which water-particle velocities were measured: one for each of the four spectra without the current, one for each spectrum with the current, and one for the current alone. This last record provided information on the amount of turbulence present in the current.

DATA ANALYSIS

Each test record contained data from five channels: three from the wave gages and two from measurements of the horizontal and vertical components of water-particle velocity. The time series were digitized at a rate of 20 Hz, each containing 12,000 data points, and were subjected to spectral analysis. Both segmental and frequency smoothing were employed for the calculation of spectral estimates. First, a series was divided into 20 segments of 512 points and spectral estimates were obtained from each segment. Then, corresponding estimates for each frequency were summed and averaged. Finally, a 5-point frequency smoothing was applied to the resulting values, the total number of degrees of freedom of the final estimates being 200.

The observed spectra of free-surface displacement for waves propagating against the current were compared with predicted spectra. The predicted spectra were derived from the observed spectra of waves on quiescent water. Two theoretical formulations were used: one based solely on Eq. 12 and the other incorporating the equilibrium range constraint, Eq. 14. The value of the constant A^* was derived by a least-squares fit to the observed data.

The observed spectra of horizontal water-particle velocity for the waves on the current were also compared with theoretical predictions derived by multiplying the theoretical free-surface displacement spectra by the appropriate values of the transfer function given in Eq. 15. However, in this case, it was also necessary to make an allowance for the presence of the turbulence in the current.

The total current velocity, $U(t)$, could be represented as follows:

$$U(t) = U + U'(t) \dots \dots \dots (19)$$

in which U = the mean current velocity; and $U'(t)$ = the fluctuating, or turbulent, component. The theoretical expressions for the particle kinematics spectra for waves on currents do not allow for the second term in the preceding expression; in the present experiments $U'(t)$ had values up to about 7% of U . Thus, each measured spectrum of horizontal water-particle velocity consisted of three parts: the first part was expressed by Eq. 15, the second was the result of weak interactions between waves and turbulence, and the third part was, purely, the autospectrum of turbulence. By subtracting this last element, which could be measured separately (see Experimental Procedure), from the total spectrum, agreement between theory and experimental results could be expected to improve. This procedure was followed.

Finally, the significant wave height, H_s , and the average zero-crossing period, T_z , were directly determined from each experimental record of free-surface displacement. The values of H_s and T_z were compared with estimates from the spectra given by:

$$H_s \approx 4(m_0)^{1/2} \dots \dots \dots (20)$$

and

$$T_z \approx 2\pi \left(\frac{m_0}{m_2} \right)^{1/2} \dots \dots \dots (21)$$

in which $m_n = \int_0^\infty \omega^n S_{\eta\eta}(\omega, U) d\omega$.

DISCUSSION

Fig. 3 shows an example of the observed spectral densities of free-surface displacement for waves on quiescent water and on the opposing current, plotted together with the theoretical values derived from Eqs. 12 and 14. The results show that Eq. 12 agrees well with the experimental data for frequencies below the spectral peak while Eq. 14 provides reasonable agreement in the equilibrium range where Eq. 12 grossly overpredicts values. However, the experiment shows spectral values re-

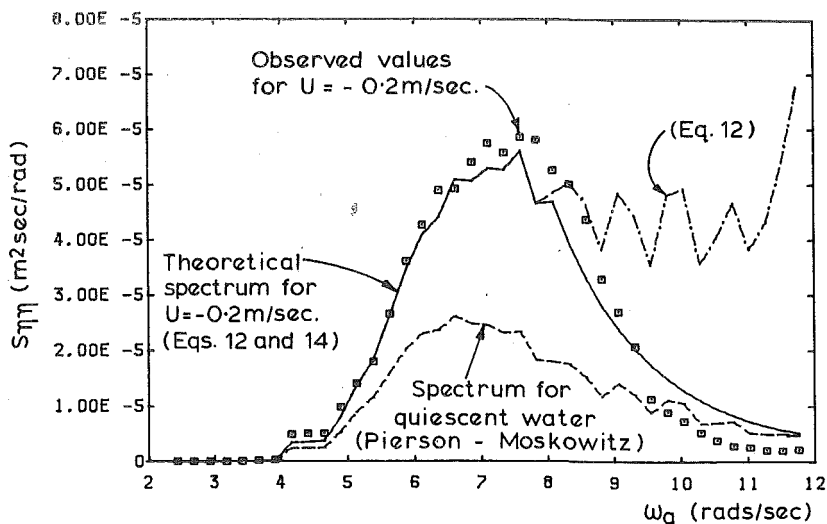


FIG. 3.—Observed and Theoretical Spectra of Free-Surface Displacement at Wave Gage 2

ducing rather more rapidly towards the higher frequencies than is predicted by the theory.

The value of A^* used in Fig. 3 is 0.0314. This value relates to a position relatively close to the point where the waves encounter the opposing

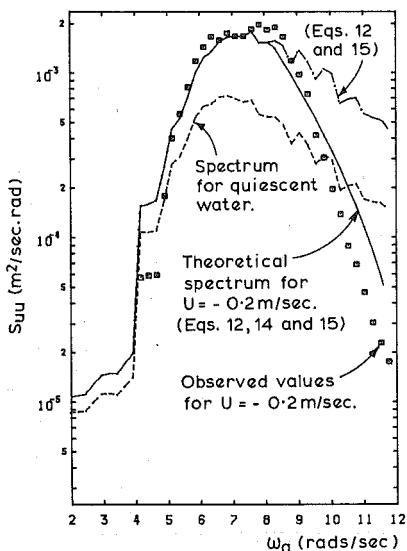


FIG. 4.—Observed and Theoretical Spectra of Horizontal Water-Particle Velocity at $z = -50$ mm

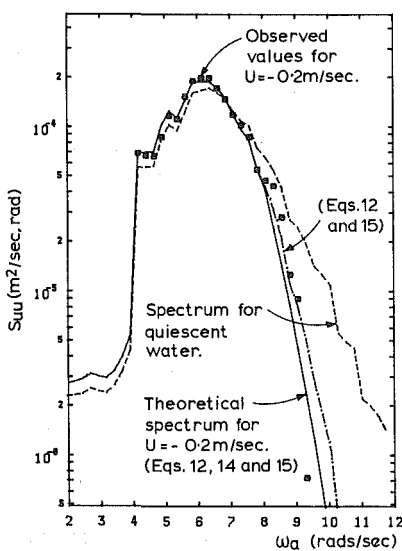


FIG. 5.—Observed and Theoretical Spectra of Horizontal Water-Particle Velocity at $z = -225$ mm

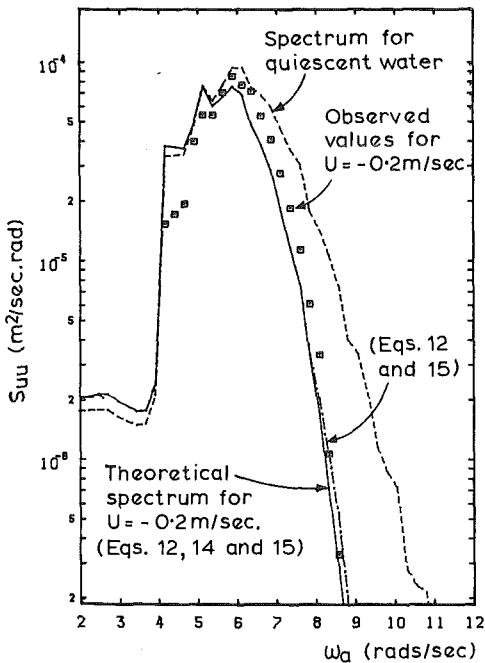


FIG. 6.—Observed and Theoretical Spectra of Horizontal Water-Particle Velocity at $z = -400$ mm

current; A^* might be expected to fall as more interactions take place between the steepened waves as they continue down the flume. Analysis of the wave-gage data for the position 10 m from the wave-maker supports this view. Additional experiments are planned in a new, longer wave/current facility to further investigate this behavior.

Figs. 4, 5 and 6 show the observed spectra of horizontal water-particle velocity. The theoretical spectra are also shown as described earlier. For $z = -50$ mm, observed values of $S_{uu}(\omega_a, U)$ below the spectral peak are predicted well by Eqs. 12 and 15, while Eqs. 14 and 15 provide reasonable predictions at higher frequencies. Again, use of Eq. 12 in the equilibrium range grossly overpredicts values. Note, however, that for $z = -225$ mm, the error in using Eq. 12 is much less; and for $z = -400$ mm the experimental data is fitted as well by Eqs. 12 and 15 as by Eqs. 14 and 15. Note also, for $z = -400$ mm, that the observed spectral densities for the waves on the current are significantly lower than the corresponding values for waves on quiescent water. This effect arises mainly as a result of the shortening of the waves by the opposing current (water-particle velocities associated with short waves decay more rapidly with depth than velocities associated with long waves).

Fig. 7 shows experimental values for the ratio of the significant wave height on the current to its value on quiescent water. These are compared with theoretical values of the ratio derived from the predicted spectra for waves on currents given by Eqs. 12 and 14. While it is risky

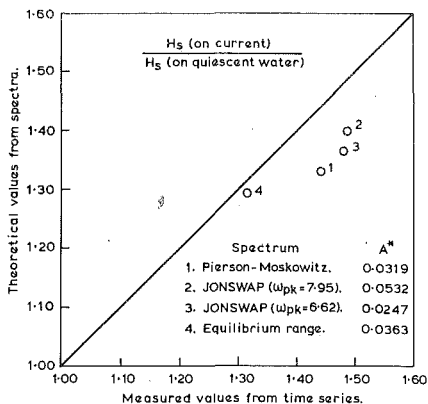


FIG. 7.—Comparison of Theoretical and Measured Changes in H_s

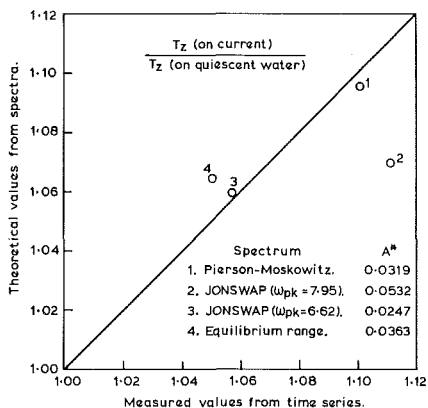


FIG. 8.—Comparison of Theoretical and Measured Changes in T_z

to draw firm conclusions on the basis of only four results, agreement between theory and experimental results appears to be good. Fig. 8 shows a similar plot for zero-crossing periods.

CONCLUSIONS

1. The theory outlined in this paper (summarized in Eqs. 12 and 14) provides reasonable predictions of the changes in the variance spectra of free-surface displacement produced by a current. The theory relates to currents which are steady and vertically uniform.

2. A feature of the theory is the allowance made for the limit on spectral densities associated with frequencies in the equilibrium range (Eq. 14). It has been shown that failure to apply the equilibrium range constraint may result in considerable overestimation of spectral values.

3. Further work is needed to investigate the factors influencing the magnitude of the empirical constant A^* .

4. The theory provides good agreement (through Eq. 15) with measurements of the spectra of horizontal water-particle velocities. The errors which arise from ignoring the equilibrium range constraint are much smaller for well-submerged points than for points close to the free surface.

5. The theory provides good estimates of the changes in H_s and T_z induced by a current, at least for the conditions covered by the present experiments.

ACKNOWLEDGMENT

This work forms part of the project, "Particle Dynamics in Non-Linear Water Waves," funded by the Science and Engineering Research Council through the North Western Universities Consortium for Marine Technology (now Marinotech North West).

APPENDIX I.—REFERENCES

1. Bretherton, F. P., and Garrett, C. J. R., "Wavetrains in Inhomogeneous Moving Media," *Proceedings of the Royal Society*, London, England, Series A, Vol. 302, No. 1471, Jan., 1968, pp. 529-554.
2. Borgman, L. E., "Ocean Wave Simulation for Engineering Design," *Journal of the Waterways and Harbors Division*, ASCE, Vol. 95, No. WW4, Nov., 1969, pp. 557-583.
3. Hedges, T. S., "Some Effects of Currents on Wave Spectra," *Proceedings of the First Indian Conference in Ocean Engineering*, Indian Institute of Technology, Madras, Vol. 1, Feb., 1981, pp. 30-35.
4. Hedges, T. S., Burrows, R., and Mason, W. G., "Wave-Current Interaction and its Effect on Fluid Loading," *Report No. MCE/3/79*, Department of Civil Engineering, University of Liverpool, Dec., 1979.
5. Huang, N. E., et al., "Interactions between Steady Non-Uniform Currents and Gravity Waves with Applications for Current Measurements," *Journal of Physical Oceanography*, Vol. 2, No. 4, Oct., 1972, pp. 420-431.
6. Jonsson, I. G., "Energy Flux and Wave Action in Gravity Waves Propagating on a Current," *Journal of Hydraulic Research*, Delft, The Netherlands, Vol. 16, No. 3, 1978, pp. 223-234.
7. Jonsson, I. G., and Wang, J. D., "Current-Depth Refraction of Water Waves," *Ocean Engineering*, Oxford, England, Vol. 7, No. 1, 1980, pp. 153-171.
8. Longuet-Higgins, M. S., and Stewart, R. W., "The Changes of Amplitude of Short Gravity Waves on Steady Non-Uniform Currents," *Journal of Fluid Mechanics*, Cambridge, England, Vol. 10, No. 4, June, 1961, pp. 529-549.
9. Longuet-Higgins, M. S., and Stewart, R. W., "Radiation Stresses in Water Waves; a Physical Discussion with Applications," *Deep-Sea Research*, Oxford, England, Vol. 11, No. 4, Aug., 1964, pp. 529-562.
10. Peregrine, D. H., "Interaction of Water Waves and Currents," *Advances in Applied Mechanics*, Vol. 16, Academic Press, New York, 1976, pp. 9-117.
11. Phillips, O. M., *The Dynamics of the Upper Ocean*, 2nd Ed., Cambridge University Press, Cambridge, England, 1977.
12. Tayfun, M. A., Dalrymple, R. A., and Yang, C. Y., "Random Wave-Current Interactions in Water of Varying Depth," *Ocean Engineering*, Oxford, England, Vol. 3, 1976, pp. 403-420.

APPENDIX II.—NOTATION

The following symbols are used in this paper:

- A = parameter in JONSWAP spectrum;
 A^* = parameter associated with spectrum equilibrium range for waves on current;
 C_{g0} = wave group velocity in zero-current region;
 C_{gr} = wave group velocity relative to current;
 d = water depth;
 E = wave energy density ($=\rho gH^2/8$);
 E_0 = wave energy density in zero-current region;
 g = gravitational acceleration;
 H = wave height;
 H_s = significant wave height (average height of highest one-third of waves in random sea);
 k = wave number ($=2\pi/L$);
 k_0 = wave number in zero-current region;
 L = wavelength;
 m_n = n th spectral moment;
 r = parameter in JONSWAP spectrum;
 $S_{\eta\eta}(\omega_a)$ = spectral density of free-surface displacement for zero-current region;
 $S_{\eta\eta}(\omega_a, U)$ = spectral density of free-surface displacement for current region;
 $S_{\eta\eta ER}(\omega_a, U)$ = limiting value of $S_{\eta\eta}(\omega_a, U)$ associated with equilibrium range;
 $S_{uu}(\omega_a, U)$ = spectral density of horizontal water-particle velocity for current region;
 T_z = average zero-crossing period;
 t = time;
 U = mean current velocity;
 $U(t)$ = total current velocity;
 $U'(t)$ = turbulent component of total current velocity;
 u_a = horizontal component of water-particle velocity in stationary frame of reference;
 u_r = horizontal component of water-particle velocity relative to current;
 W = wind speed;
 x = horizontal distance, in direction of wave propagation, from origin of stationary co-ordinate system;
 x_r = horizontal distance, in direction of wave propagation, from origin of co-ordinate system moving with current;
 z = vertical distance, positive upwards, from mean-water-level;
 γ = parameter in JONSWAP spectrum (the peak enhancement factor);
 η = displacement of water surface from mean-water-level;
 π = 3.14159 ...;
 ρ = water density;

- σ = parameter in JONSWAP spectrum;
- ω_a = wave angular frequency in stationary frame of reference (apparent wave angular frequency);
- ω_r = wave angular frequency in frame of reference moving with current (intrinsic wave angular frequency); and
- ω_{pk} = value of ω_a associated with peak of JONSWAP spectrum.